# A Power Electronic Transformer based on Indirect Matrix Converter for PWM AC Drive with Lossless Commutation of Leakage Energy

***Arushi Shahani*, Kaushik Basu and Ned Mohan***

**University of Minnesota, 200 Union Street SE Minneapolis-55455 USA, email: shah0379@umn.edu*

**Keywords:** high frequency ac link, power electronic transformer, lossless commutation of leakage energy, indirect matrix

## Abstract

High frequency ac link three phase ac to three phase adjustable speed and magnitude PWM ac converters with single stage power conversion and bidirectional power flow are important in the generation of power from renewable energy sources or where isolation is necessary. Due to the use of high frequency these type of converters achieve high power density. Open loop power factor correction, higher efficiency and reliability are important features of these type of converters. One major problem in this type of converter is the commutation of leakage energy which results in power loss, reduction in switching frequency, distortion and loss of output voltage. The topology based on the indirect modulation of matrix converters uses minimum amount of copper and has relatively less number of semiconductor switches. This paper presents a lossless source based commutation strategy along with a modulation technique that minimizes the frequency of leakage inductance commutation. It also results in the soft switching of the output converter (Zero current switching : ZCS). The topology along with the proposed control has been analysed and simulated. Simulation results confirm the operation.

## 1 Introduction

Three phase ac to ac converters with a high frequency ac link find application in generation of power from renewable energy sources such as wind [1]. Generally power is generated at a comparatively low voltage level and a line frequency transformer is used to connect to the high voltage grid. Replacement of line frequency transformer with one having a higher frequency leads to considerable reduction in size, weight and hence increases the power density of the system. The high frequency transformer provides a flexible voltage transfer ratio in addition to the usual advantage of galvanic isolation. High frequency ac link ac/ac topologies with single stage power conversion and bidirectional power flow obviates any need for the use of passive components such as a dc link capacitor and hence increasing the reliability of the system [2], [3]. According to [4] these converters can be classified into three groups. One problem in this type of converters is the presence of leakage inductance in the high frequency transformer windings. Commutation of leakage inductance current leads to the distortion of the output current waveform, output voltage loss and reduction in the frequency of operation [5]. Use of a snubber circuit for commutation results in power loss. [6]. For the third group of converters as mentioned in [4], a lossless source based commutation method has been developed along with a control strategy that minimizes the frequency of leakage inductance commutation. One of the problems in these converters is the usage of increased number of semi-conductor switches, 32 (two quadrant) in [6] and 48 in [7]. Converters in group 2, as mentioned in [4], uses minimum number of semiconductor switches. The converter with minimum switch count (20) was presented in [8]. It is shown in [9] [10] that for this converter source based commutation is not possible and secondary side snubber circuit is necessary. Converter topologies for group 1 as given in [4], are based on the indirect modulation of matrix converters. The topology(from group 1) used in this paper was originally presented in [11]. An advantage of this topology is that it uses a single phase transformer in comparison with three transformers used in the converters from other two groups. It also uses one third less amount of copper. The number of switches used (24) is comparable to that of topologies from group 2. The leakage inductance commutation problem for this type of converters in noted in [12]. In this paper a lossless source based commutation method has been developed based on a similar technique originally proposed in [13]. This leads to soft switching of the output converter (ZCS). A novel modulation technique has been developed in order to minimize the frequency of the leakage inductance commutation in this topology. In section II the proposed modulation method and the source based commutation technique are described in detail. Section III presents the relevant simulation results.

## 2 Analysis

In this section a novel switching strategy based on the control of the indirect matrix converter has been presented for a three phase ac-ac converter with a high frequency transformer as shown in Fig. 1. This circuit consists of two converters. The

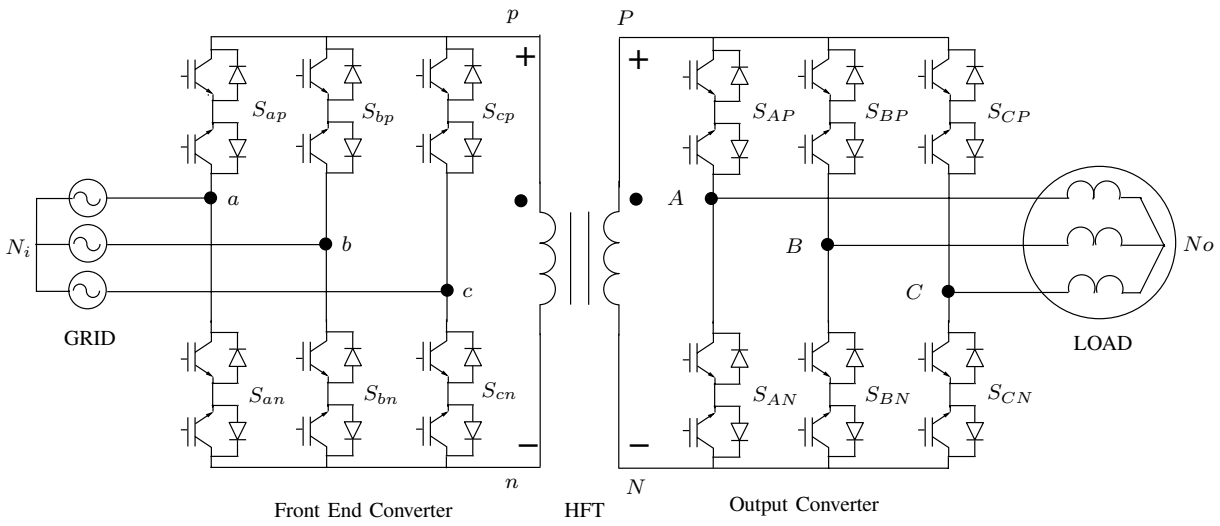


Fig. 1. Circuit diagram of the power electronic converter system

front end converter which converts an input three phase utility to a high frequency single phase ac. This converter works as a current source inverter (CSI) and the fundamental component of input currents are shaped to obtain unity power factor. The output of the front end converter is fed to a single phase high frequency transformer (HFT). Secondary of the HFT is connected to the output converter. The output converter functions as a voltage source inverter (VSI) and converts the single phase ac to a balanced three phase voltage of desired magnitude and frequency. This converter uses four quadrant switches with common emitter connection of two IGBTs.

The working of this converter is divided into two parts, one being the synthesis of the output voltage with appropriate modulation scheme and the other being the commutation of the leakage energy.

### 2.1 Modulation of the Front End Converter

The front end converter is modulated as a current source inverter. Three phase balanced line to neutral voltages are given by (1), where $V_{IN}$ is the peak of the input voltage and $\omega_i$ is the input frequency. Fundamental components of the input line currents are given by (2). Input line current space vector is defined in (3). (4) gives the input line current space vector, $\bar{\mathbf{I}}_{in}$, averaged over a sampling period $T_s$. The input converter is switched in such a way that the average input line current space vector is in phase with the input voltage space vector. This results in unity power factor. Fig. 2 shows the current space vectors produced by the input side converter for various allowable switching states. Switching state [a,b] in Fig. 2, refers to the state when the switches $S_{ap}$ and $S_{bn}$ are on in Fig. 1. The position of the average input current vector to be synthesized by the input converter is obtained by sensing the input line voltages. Modulation index $m_I$ of this converter is defined in (5). It is set to its maximum value of one. $I_{dc,virtual}$ is the dc component of the virtual dc link current. (6) gives the duty ratios of the two active switching states to be applied over one sampling cycle depending on the position of $\bar{\mathbf{I}}_{in}$. For example, as shown in Fig. 2, the two active states [a,b] ($\mathbf{I_1}$) and [a,c] ($\mathbf{I_2}$) will be applied for $dI_1$ and $dI_2$ fractions of time respectively.

$$\begin{aligned} v_{aN_i} &= V_{IN}\cos\omega_i t \\ v_{bN_i} &= V_{IN}\cos\left(\omega_i t - \frac{2\pi}{3}\right) \\ v_{cN_i} &= V_{IN}\cos\left(\omega_i t + \frac{2\pi}{3}\right) \end{aligned} \tag{1}$$

$$\begin{aligned} \bar{i_a} &= I_{IN}\cos\omega_i t \\ \bar{i_b} &= I_{IN}\cos\left(\omega_i t - \frac{2\pi}{3}\right) \\ \bar{i_c} &= I_{IN}\cos\left(\omega_i t + \frac{2\pi}{3}\right) \end{aligned} \tag{2}$$

$$\mathbf{I}_{in} = i_a + i_b e^{\frac{j2\pi}{3}} + i_c e^{-\frac{j2\pi}{3}} \tag{3}$$

$$\bar{\mathbf{I}}_{in} = \frac{3}{2} I_{IN} e^{j\omega_i t} \tag{4}$$

$$m_I = \left(\frac{I_{IN}}{I_{dc,virtual}}\right) \tag{5}$$

$$\begin{aligned} dI_1 &= m_I \sin\left(\frac{\pi}{3} - \beta\right) \\ dI_2 &= m_I \sin\beta \end{aligned} \tag{6}$$

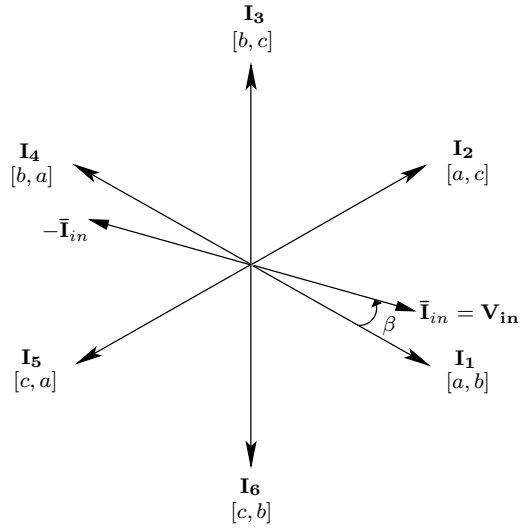


Fig. 2. Current space vectors produced by the front end converter

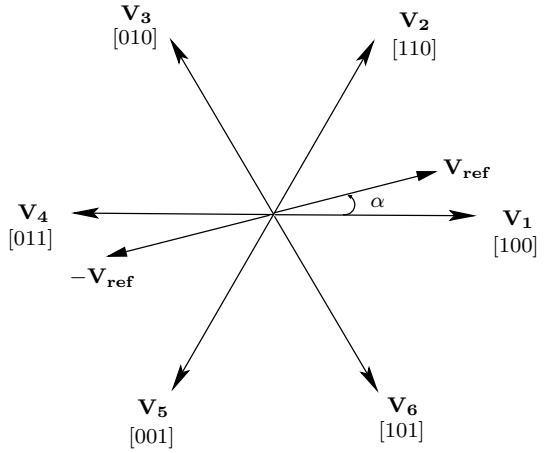


Fig. 3. Voltage space vectors produced by the output converter

### 2.2 Modulation of the Output Converter

The output converter first rectifies the high frequency ac (virtual dc link voltage chopped with 50% duty cycle) and then inverts it to an adjustable speed and magnitude three phase ac for the output load. As a two level inverter, the output converter can be switched to eight unique states. (7) defines the output voltage space vector. Fig. 3 shows the voltage space vectors produced by the output converter. Switching state [100] in Fig. 3, refers to the state when the switches $S_{AP}$, $S_{BN}$ and $S_{CN}$ are on as shown in Fig. 1. (8) gives average three phase balanced line to neutral voltages with $V_o$ as the peak and $\omega_o$ as the frequency. This results in a constant magnitude synchronously rotating average output voltage vector $\mathbf{V_{ref}}$ to be generated by switching the output converter, (9). Modulation index $m_V$ of output converter is defined in (10) and is set to $\frac{2V_o}{3V_i}$ in order to generate the required output voltage. $V_{dc,virtual}$ is the dc component of the virtual dc link voltage. (11) gives the duty ratios of the two active switching states to be applied over one sampling cycle depending on the position of the average output voltage vector. For example, as shown in Fig. 3, the two active states [100] ($\mathbf{V_1}$) and [110] ($\mathbf{V_2}$) will be applied for $dV_1$ and $dV_2$ fractions of time respectively.

$$\mathbf{V_o} = v_{AN_o} + v_{BN_o}e^{\frac{j2\pi}{3}} + v_{CN_o}e^{-\frac{j2\pi}{3}} \tag{7}$$

$$\begin{aligned}
\bar{V}_{AN} &= V_o \cos(\omega_o t + \phi_o) \\
\bar{V}_{BN} &= V_o \cos\left(\omega_o t - \frac{2\pi}{3} + \phi_o\right) \\
\bar{V}_{CN} &= V_o \cos\left(\omega_o t + \frac{2\pi}{3} + \phi_o\right)
\end{aligned} \tag{8}$$

$$\begin{aligned}
\mathbf{V_{ref}} &= \bar{v}_{AN_o} + \bar{v}_{BN_o}e^{\frac{j2\pi}{3}} + \bar{v}_{CN_o}e^{-\frac{j2\pi}{3}} \\
&= \frac{3}{2}V_o e^{j(\omega_o t + \phi_o)}
\end{aligned} \tag{9}$$

$$m_V = \frac{V_o}{V_{dc,virtual}} \tag{10}$$

$$\begin{aligned}
dV_1 &= \sqrt{3}m_V \sin\left(\frac{\pi}{3} - \alpha\right) \\
dV_2 &= \sqrt{3}m_V \sin\alpha
\end{aligned} \tag{11}$$

### 2.3 Combined modulation of the input and output Converter

Switching transition of the secondary side converter results in the commutation of the leakage energy. The objective of the modulation strategy developed in this paper is to minimize the number of switching of the output converter over a sampling cycle. As shown in Fig. 4, a sawtooth carrier $C_1$ is used to generate pulses for the output converter ($SV_1$ and $SV_2$). Vector $\mathbf{V_1}$ is applied for $dV_1$ fraction of time and $\mathbf{V_2}$ is applied for remaining time period. While the zero vector is applied by using the input converter. Variable slope carriers $C_2$ and $C_3$ are generated from the signals $SV_1$ and $SV_2$. $dI_1$ is compared with $C_2$ in order to generate the signal $SI_1$ (when high vector $\mathbf{I_1}$ is applied by the input converter). Similarly $SI_2$ is generated using the carrier $C_3$ and $dI_2$. This modulation scheme ensures minimum switching of the output converter.

The signal $S$, as shown in Fig. 5, controls the flux balance in the converter. $S$ is a square wave with 50% duty cycle which is synchronized with the carrier $C_1$ of Fig. 4 at half of its frequency. When $S$ is high $v_{pn}^{-} = V_{dc,virtual}$, $i_{pn}^{-} = I_{dc,virtual}$ and the modulation of the converter is done by the application of vectors $\mathbf{I_1}$, $\mathbf{I_2}$, $\mathbf{V_1}$ and $\mathbf{V_2}$. When $S$ is low $i_{pn}^{-} = -I_{dc,virtual}$ and in order to generate same $\mathbf{I}_{in}$ we need to apply $\mathbf{I_4}$ and $\mathbf{I_5}$ in the input converter, this is equivalent

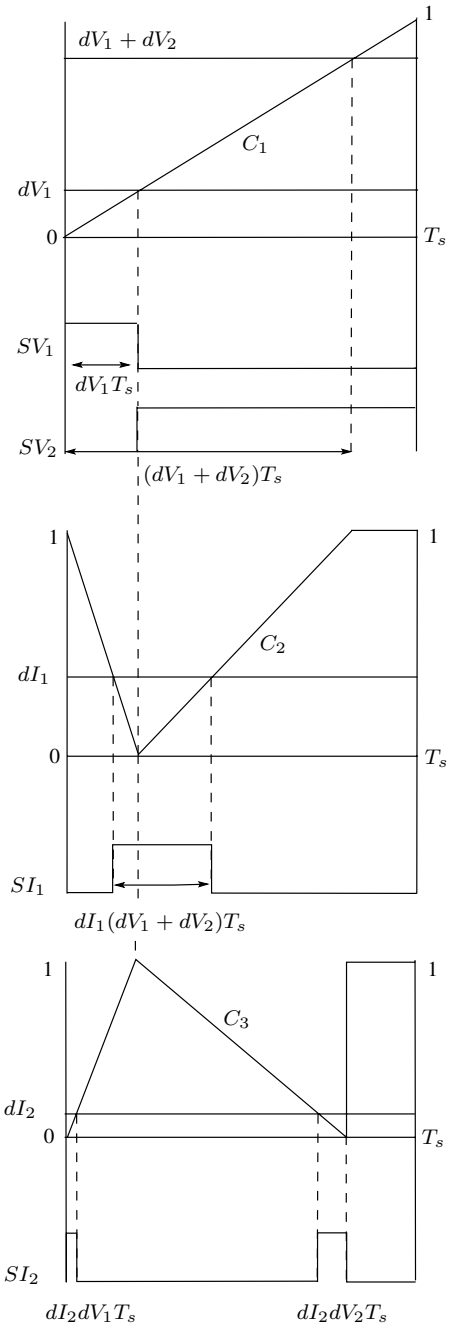


Fig. 4. Signal generation for combined modulation

to reversing the reference input current vector. Same is true for the output converter. This results in flux balance in the transformer core over one complete cycle of $S$.

### 2.4 Commutation

Commutation refers to the process of changing the current flowing through the leakage inductance of the transformer when the output converter is switched. In this analysis the magnetizing inductance of the transformer is neglected and it is modeled as a series connection of primary and secondary leakage inductances ($L_{lkg}$). The output load is inductive in

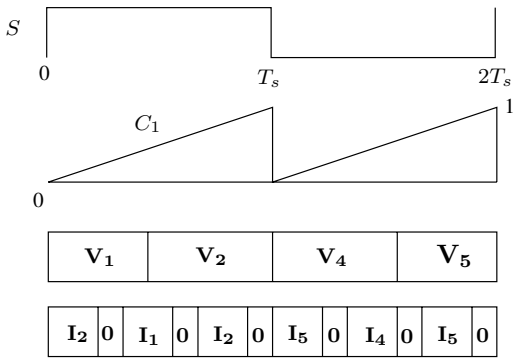


Fig. 5. Flux balance

nature and any switching transition of the secondary side converter requires a change in the current flowing through $L_{lkg}$. During the switching state change in the output converter, only one leg is switched at a given instant of time i.e. transition from $\mathbf{V_1}$ to $\mathbf{V_2}$ implies switching of leg B. Similarly while transiting from $\mathbf{V_2}$ to $\mathbf{V_4}$, $\mathbf{V_3}$ is applied as an intermediate state.

The commutation strategy presented in this paper utilizes the input source voltages to commute the current in $L_{lkg}$. Depending on the direction of the flow of the load current (of the phase connected to the leg undergoing switching) and the type of switching (from bottom to top or vice versa) there are four possible cases and one of them has been described in detail. As the commutation time is very small compared to the time periods of the input voltage and the output current waveforms, during commutation it is possible to assume that the output currents and the input voltages can be represented as dc sources (ie $i_A$ as $I_A$ and $v_a$ as $V_a$) as shown in Fig (6). Lets assume leg B is switching from top to bottom (transition from $\mathbf{V_2}$ to $\mathbf{V_1}$) and $I_B$ is positive. Initially $i_{lkg} = I_A + I_B$. At the beginning of commutation process $Q_2$ is turned off (the non conducting IGBT in the bidirectional switch pair $Q_1$, $Q_2$). There after the IGBT that will be conducting in the upcoming switching state is turned on i.e. $Q_4$. In the final stage $i_{lkg}$ must become $I_A$. This implies that the current through $L_{lkg}$ should decrease ($I_B > 0$). The maximum negative line to line voltage (say $V_{ca}$) available at that instant of time is applied through the input converter. This forward biases the diode $D_3$ and the current through $L_{lkg}$ starts decreasing (as $V_{ca} = L_{lkg}\frac{di_{lkg}}{dt}$). As the current through diodes $D_2$ and $D_3$ can not reverse, when $i_{lkg}$ becomes equal to $I_A$ the commutation process comes to a natural end. We wait in this state for $t_{com}$ amount of time as given in (12). This is the estimated maximum commutation time. Thereafter $Q_1$ is turned off and $Q_3$ is turned on. Note that the switching of $Q_{1,2,3,4}$ happens with zero current (ZCS).

$$t_{com} = \frac{L_{lkg}I_o}{1.5V_{in}} \tag{12}$$

| | |
|---|---|
| $V_i$ | $500\sqrt{2}V$ |
| $R_{load}$ | $8\Omega$ |
| $L_{load}$ | $12.7mH$ |
| $L_{lkg}$ | $100\mu H$ |
| $L_m$ | $10\ mH$ |
| $\frac{N_2}{N_1}$ | 1 |
| $f_s = \frac{1}{T_s}$ | 5kHz |
| $\omega_o$ | $2\pi 60$ |
| $\omega_i$ | $2\pi 60$ |
| $m_I$ | 1 |
| $m_V$ | 0.4 |

Table 1: Parameters

## 3 Simulation

The topology in Fig. (1) along with the proposed control has been simulated in MATLAB/Simulink. The parameters for the simulation are given in Table 1. Fig. 7 shows simulated output line to neutral voltage and line current of phase $A$. The peak of the output line current is slightly lower than its analytically predicted value (Analytical $I_A = 22.73A$, Simulated $I_A = 21.4A$). This is due to the loss of output voltage during commutation. Fig. 8 shows the filtered input current in phase $a$ along with the corresponding input line to neutral voltage hence verifying input power factor correction. Fig. 9 presents commutation of leakage inductance current when the output converter is making a transition from [011] to [001]. In Fig. 9.a. leg B is switching from top to bottom The leakage inductance current linearly changes from $I_B + I_C = -22A$ to $I_C = -8.5A$, Fig. 9.b. The slope of the linear rise matches with analytical predictions. This change in the current $i_{lkg}$ requires a positive $V_{PN}$, Fig. 9.c. $V_{ac} = 1225V$ was the maximum line to line voltage at that instant of time. The

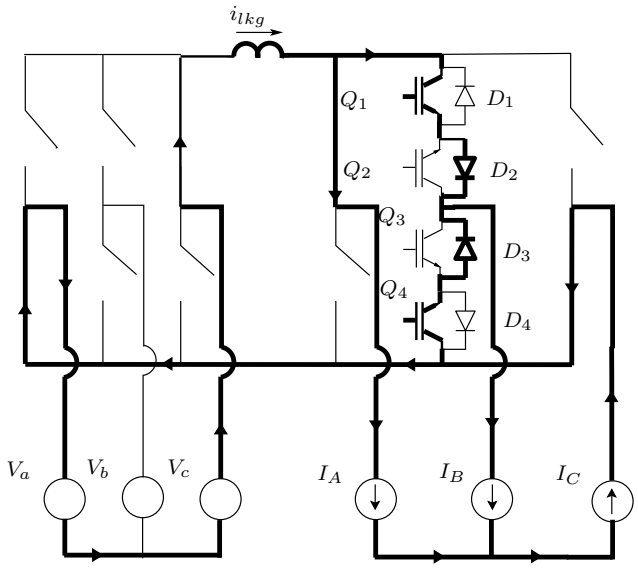


Fig. 6. Commutation

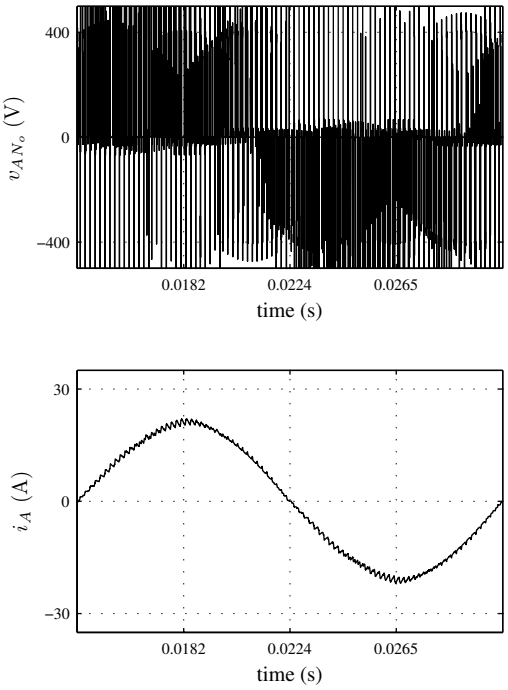


Fig. 7. Simulation result: a) output line to neutral voltage b) output line current

magnetising current of the transformer over two cycles of $S$ is shown in Fig. 10. This verifies flux balance.

## 4 Conclusion

The ac/ac power electronics transformer topology based on the indirect modulation of matrix converter has the following advantages 1) high power density 2) isolation 3) single stage power conversion 4) input power factor correction 5) less number of semiconductor switches (equal in primary as well as secondary side) 6) and uses minimum amount of copper. In this paper a novel modulation method along with a commutation technique has been proposed. This not only preserves all of the previously mentioned advantages but also results in a) lossless commutation in leakage energy b) soft switching of output converter (ZCS) c) minimization of the frequency of leakage inductance commutation leading to less output voltage loss and increased frequency of operation. The topology along with the proposed control technique has been analysed and simulated. Simulation results confirm the advantages.

## References


[1] R. K. Gupta, G. F. Castelino, K. K. Mohapatra, and N. Mohan, "A novel integrated three-phase, switched multi-winding power electronic transformer converter for wind power generation system," in *Proc. Industrial Electronics Society, 2009. IECON'09. The 35th Annual Conference of the IEEE*, Porto, Portugal, Nov. 2009.

[2] M. Kang, P. Enjeti, and I. Pitel, "Analysis and design of electronic transformers for electric power distribution system," in *Industry Applications Conference, 1997. Thirty-Second IAS Annual Meeting, IAS '97., Conference Record of the 1997 IEEE*, vol. 2, Oct 1997, pp. 1689–1694 vol.2.

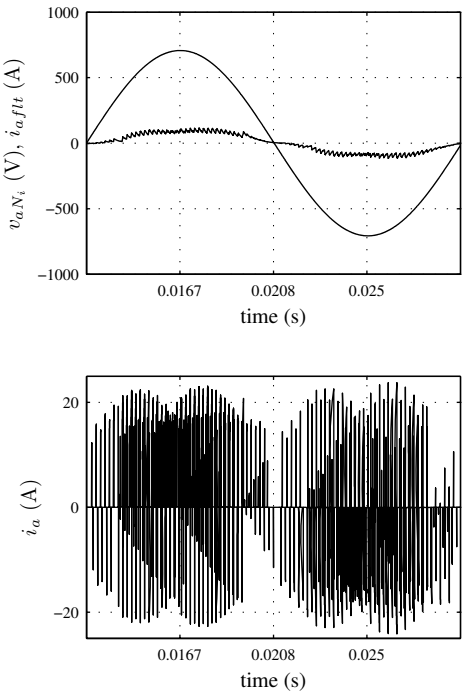


Fig. 8. Simulation result: a) input line to neutral voltage with filtered input line current (20A/div) b) actual input line current

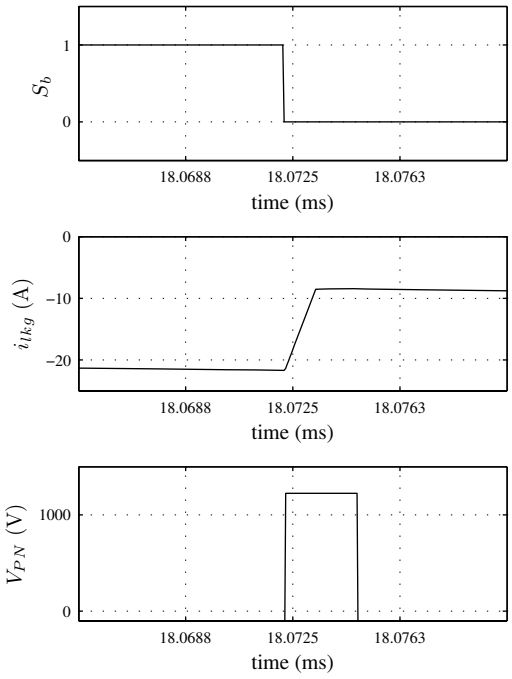


Fig. 9. Simulation result: commutation

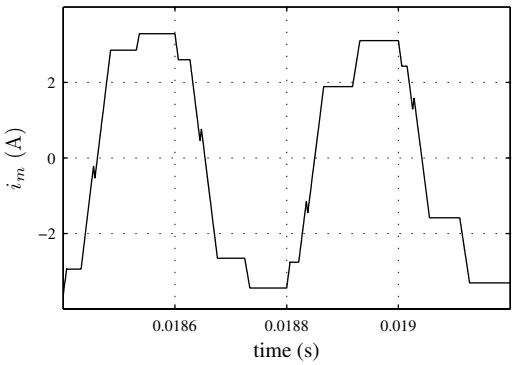


Fig. 10. Simulation result: magnetizing current


[3] D. Chen and J. Liu, "The uni-polarity phase-shifted controlled voltage mode ac-ac converters with high frequency ac link," *Power Electronics, IEEE Transactions on*, vol. 21, no. 4, pp. 899–905, July 2006.

[4] K. Basu, R. K. Gupta, S. Nath, G. F. Castelino, K. K. Mohapatra, and N. Mohan, "Research in matrix-converter based three-phase power-electronic transformers," in *Power Electronics Conference (IPEC), 2010 International*, jun. 2010, pp. 2799 –2803.

[5] S. Nath, K. Mohapatra, and N. Mohan, "Output voltage regulation in matrix converter fed power electronic transformer for power systems application in electric ship," in *Electric Ship Technologies Symposium, 2009. ESTS 2009. IEEE*, april 2009, pp. 203 –206.

[6] K. Basu, A. Somani, K. Mohapatra, and N. Mohan, "A three-phase ac/ac power electronic transformer-based pwm ac drive with lossless commutation of leakage energy," in *Power Electronics Electrical Drives Automation and Motion (SPEEDAM), 2010 International Symposium on*, june 2010, pp. 1693 –1699.

[7] K. Basu and N. Mohan, "A power electronic transformer for three phase pwm ac/ac drive with loss less commutation and common-mode voltage suppression," in *IECON 2010 - 36th Annual Conference on IEEE Industrial Electronics Society*, nov. 2010, pp. 315 –320.

[8] R. K. Gupta, K. K. Mohapatra, and N. Mohan, "A novel three-phase, switched multi-winding power electronic transformer," in *Proc. IEEE Energy Conversion Congress and Exposition (ECCE) 2009*, San Jose, CA, Sep. 2009, pp. 2696 –2703.

[9] G. Castelino, K. Basu, R. Gupta, and N. Mohan, "Power electronic transformer with reduced number of switches: Analysis of input clamp circuit and a modulation strategy to eliminate input snubber requirement," in *IECON 2010 - 36th Annual Conference on IEEE Industrial Electronics Society*, nov. 2010, pp. 656 –661.

[10] G. Castelino, K. Basu, and N. Mohan, "Power electronic transformer with reduced number of switches: Analysis of clamp circuit for leakage energy commutation," in *Power Electronics, Drives and Energy Systems (PEDES) 2010 Power India, 2010 Joint International Conference on*, dec. 2010, pp. 1 –8.

[11] H. Cha and P. Enjeti, "A three-phase ac/ac high-frequency link matrix converter for vscf applications," in *Power Electronics Specialist Conference, 2003. PESC '03. 2003 IEEE 34th Annual*, vol. 4, June 2003, pp. 1971–1976 vol.4.

[12] K. Basu, A. Umarikar, K. Mohapatra, and N. Mohan, "High-frequency transformer-link three-level inverter drive with common-mode voltage elimination," in *Power Electronics Specialists Conference, 2008. PESC 2008. IEEE*, June 2008, pp. 4413–4418.

[13] M. Matsui, M. Nagai, M. Mochizuki, and A. Nabae, "High-frequency link dc/ac converter with suppressed voltage clamp circuits-naturally commutated phase angle control with self turn-off devices," *Industry Applications, IEEE Transactions on*, vol. 32, no. 2, pp. 293–300, Mar/Apr 1996.